

*This is the pre-peer reviewed version of the following article: “Read, J., Delhayé, E., & Sougné, J. (2023). Computational models can distinguish the contribution from different mechanisms to familiarity recognition. *Hippocampus*, 1–15” which has been published in final form at <https://doi.org/10.1002/hipo.23588>. This article may be used for non-commercial purposes in accordance with Wiley Terms and Conditions for Use of Self-Archived Versions.*

1           **Computational models can distinguish the contribution from different**  
2   **mechanisms to familiarity recognition**

3   John Read<sup>1</sup>, Emma Delhay<sup>1,2</sup> & Jacques Sougné<sup>2,3</sup>

4           <sup>1</sup> GIGA Centre de Recherche du Cyclotron In Vivo Imaging, University of Liège, Liège,  
5           Belgium, <sup>2</sup> Psychology and Cognitive Neuroscience Research Unit, University of Liège,  
6           Liège, Belgium, <sup>3</sup> UDI-FPLSE, University of Liège, Liège, Belgium

7  
8  
9  
10  
11  
12  
13  
14  
15  
16   **Corresponding author:** John Read, GIGA-CRC In Vivo Imaging, University of Liège, Liège,  
17   Belgium, Allée du Six Août, 8 (B30), Quartier Agora, 4000 Sart-Tilman, Belgium.

18   Tel.: +32 366 35 64; email: john.read@uliege.be

19   ORCID for the corresponding author: 0009-0009-3269-4362

20 **AUTHORSHIP**

21 **John Read:** Conceptualization, Methodology, Coding, Formal analysis and Data Visualization,  
22 Interpretation, Writing (original draft), Project administration. **Emma Delhaye:** Interpretation,  
23 Writing (review & editing). **Jacques Sougné:** Conceptualization, Methodology, Formal  
24 analysis, Writing (review & editing), Supervision, Project administration.

25

26

27

28

29

30

31

32

33

34

35

36

37

38 **ACKNOWLEDGMENTS**

39 The authors thank Stephan Defraire for his invaluable support throughout the coding process at  
40 the early stages of the study as well as Dr. Christine Bastin for the inspiring discussion about  
41 the behavioral part of this work. The authors also want to give a very special thanks to Dr.  
42 Daniel Defays for his help in the comprehension of the mathematics behind the algorithms, his  
43 insightful comments on the manuscript and his support throughout this entire project.

44

45

46

47

48

49

50

51

52

53

54

55

56

57 **ABSTRACT**

58 Familiarity is the strange feeling of knowing that something has already been seen in our past.  
59 Over the past decades, several attempts have been made to model familiarity using artificial  
60 neural networks. Recently, two learning algorithms successfully reproduced the functioning of  
61 the perirhinal cortex, a key structure involved during familiarity: Hebbian and anti-Hebbian  
62 learning. However, performance of these learning rules is very different from one to another  
63 thus raising the question of their complementarity. In this work, we designed two distinct  
64 computational models that combined Deep Learning and a Hebbian learning rule to reproduce  
65 familiarity on natural images, the Hebbian model and the anti-Hebbian model respectively. We  
66 compared the performance of both models during different simulations to highlight the inner  
67 functioning of both learning rules. We showed that the anti-Hebbian model fits human  
68 behavioral data whereas the Hebbian model fails to fit the data under large training set sizes.  
69 Besides, we observed that only our Hebbian model is highly sensitive to homogeneity between  
70 images. Taken together, we interpreted these results considering the distinction between  
71 absolute and relative familiarity. With our framework, we proposed a novel way to distinguish  
72 the contribution of these familiarity mechanisms to the overall feeling of familiarity. By  
73 viewing them as complementary, our two models allow us to make new testable predictions  
74 that could be of interest to shed light on the familiarity phenomenon.

75

76

77

78 **KEY WORDS:** Neural Networks (Computer), Recognition (Psychology), Perirhinal Cortex,  
79 Algorithms

## 80 INTRODUCTION

81 Recognition memory has been described as the ability to determine if one has already  
82 encountered or not an event such as an object or a person (see Besson, Ceccaldi, & Barbeau,  
83 2012 for a review article on the subject). Although it was highly debated among the scientific  
84 community, it is now commonly accepted that two retrieval processes can occur during  
85 recognition (Jacoby, 1991; Mandler, 1980; Tulving, 1985; Yonelinas, Ramey, & Riddell,  
86 2022). Familiarity-based recognition is the feeling of knowing that something – or someone –  
87 has already been seen in the past, without recall of the context in which it has been encountered  
88 (Tulving, 1985; Yonelinas, Aly, Wang, & Koen, 2010). By contrast, recollection-based  
89 recognition refers to the experience of consciously remembering an event (Tulving, 1985;  
90 Yonelinas et al., 2010). Over the past decades, *Dual Process theories* proposed that recollection  
91 and familiarity work as two functionally and anatomically independent processes (see Diana,  
92 Reder, Arndt, & Park, 2006; Eichenbaum, Yonelinas, & Ranganath, 2007; Yonelinas, 2002 for  
93 reviews).

94 Recent studies suggest that familiarity emerges through the implication of an anterior-  
95 temporal network including several brain regions (Bastin et al., 2019; Merkow, Burke, &  
96 Kahana, 2015; Ritchey, Libby, & Ranganath, 2015; Scalici, Caltagirone, & Carlesimo, 2017;  
97 Yonelinas, Otten, Shaw, & Rugg, 2005). Previous works have also shown that the perirhinal  
98 cortex (PrC) is crucial during familiarity detection (Aggleton & Brown, 2006; Bowles et al.,  
99 2010; Eichenbaum et al., 2007; Montaldi & Mayes, 2010). For example, a study showed that  
100 during a recognition task, patients with specific lesions in the PrC present impaired familiarity  
101 without recollection dysfunction (K. R. Brandt, Eysenck, Nielsen, & von Oertzen, 2016). These  
102 works were also supported by Wolk, Dunfee, Dickerson, Aizenstein, & Dekosky (2011), who  
103 showed an anatomic double dissociation between familiarity associated with the PrC and  
104 recollection associated with the hippocampus.

105           Looking more closely at patterns of neural firing during familiarity-based recognition,  
106 electrophysiological studies in monkeys showed that a small fraction of PrC neurons – called  
107 *novelty neurons* – respond in a stronger manner when new stimuli are presented (Brown &  
108 Xiang, 1998; Xiang & Brown, 1998). More importantly, this pattern of high activation tends to  
109 decrease when the same stimuli are presented again (Brown & Aggleton, 2001). In other words,  
110 when a stimulus is new, novelty neurons in the PrC will respond with a higher firing rate. But,  
111 when the same stimulus becomes familiar, its activity in the PrC is reduced compared to a novel  
112 stimulus. This phenomenon known as repetition suppression has also been observed in the  
113 human brain. This is notably the case in the inferotemporal cortex, a region which is adjacent  
114 to the PrC and is involved in visual perception (Grill-Spector, Henson, & Martin, 2006; Meyer  
115 & Rust, 2018).

116           Several works in computational modeling are grounded around Dual Process  
117 frameworks and the implication of the PrC in familiarity detection (Cowell, 2012). For example,  
118 a neurocomputational model brought evidence that human must resort to two complementary  
119 learning systems to adequately capture the mechanisms of recognition memory (Norman &  
120 O'Reilly, 2003). According to this framework, the hippocampus is involved in the recall of  
121 details from specific events (i.e., recollection) whereas the medial-temporal cortices – including  
122 the PrC – learned the statistical regularities of the environment (i.e., familiarity). Intriguingly,  
123 it seems difficult to implement these two functions in a single system (McClelland,  
124 McNaughton, & O'Reilly, 1995). Therefore, Norman & O'Reilly (2003) developed two  
125 separate networks for recognition: the hippocampal model for recollection and the neocortical  
126 model for familiarity. Basically, the neocortical model (Norman, 2010; Norman & O'Reilly,  
127 2003) encodes regularities in the input layer (i.e. a stimulus) with Hebbian learning and assigns  
128 similar representations to similar stimuli. When the same stimulus is presented repeatedly to  
129 the neocortical model, the internal representation of this stimulus will sharpen gradually and

130 fewer neurons will respond to the stimulus. However, these neurons will be strongly activated.  
131 Here, familiar stimuli will strongly activate a small number of neurons whereas novel stimuli  
132 will weakly activate many neurons. Paradoxically, the idea behind familiarity-based  
133 recognition is the ability to recognize events that only have occurred once (Yonelinas et al.,  
134 2022). This assumption seems therefore incompatible with the gradual learning postulated by  
135 the neocortical model.

136 Another major limitation of the neocortical model – as well as for other architectures –  
137 is that they used formal binary patterns (i.e., sequences of 0s and 1s) as direct inputs for  
138 memorizing (Bogacz & Brown, 2003b; Norman & O’Reilly, 2003; Sohal & Hasselmo, 2000).  
139 One could reasonably assume that this kind of inputs are not congruent with the processing  
140 occurring in human brain. As a matter of fact, our judgments of familiarity arise from events  
141 involving real stimuli instead of artificial patterns. Eichenbaum et al. (2007) proposed a  
142 functional organization for visual processing in the median temporal lobes including the PrC.  
143 In this organization, most of the neocortical input to the PrC comes from association areas called  
144 the ventral pathway (Eichenbaum et al., 2007). The ventral pathway process unimodal sensory  
145 information about qualities of objects: the so-called “*what*” information (Humphreys &  
146 Riddoch, 2006). The representation of a stimulus formed by the ventral pathway allows  
147 subsequent judgment of familiarity. Trying to fulfill the gap between modelling and human  
148 brain processing, some models used convolutional neural networks (CNN) to mimic the ventral  
149 pathway processing to the PrC (Ji-An, Stefanini, Benna, & Fusi, 2022; Kazanovich & Borisyuk,  
150 2021; Tyulmankov, Yang, & Abbott, 2022). In principle, every pre-trained CNN followed by  
151 a simple neural network could successfully model familiarity on natural images with an  
152 adequate synaptic plasticity rule (Kazanovich & Borisyuk, 2021).

153 Accordingly, two synaptic plasticity rules seem very promising to model familiarity-  
154 based recognition: the Hebbian and the anti-Hebbian learning rules (Bogacz & Brown, 2003b;



155 Tyulmankov et al., 2022). The functioning of these learning rules are based on Hebb's works  
156 (Hebb, 1949):

157 *“When an axon of cell A is near enough to excite cell B and repeatedly or persistently*  
158 *takes part in firing it, some growth process or metabolic change takes place in one or both cells*  
159 *such that A's efficiency, as one of the cells firing B, is increased.”*

160 Computational models using Hebb's theory to model familiarity are essentially designed  
161 as two-layers feedforward networks (Androulidakis, Lulham, Bogacz, & Brown, 2008; Bogacz  
162 & Brown, 2003a; Bogacz, Brown, & Giraud-Carrier, 2001b). In these networks, weight  
163 modification is implemented such as the connection strengths are either strengthened or  
164 weakened in response to co-activated neurons. The direction of this modification (i.e.,  
165 strengthening or weakening) depends on the chosen synaptic plasticity rule. Respectively, the  
166 Hebbian plasticity potentiates connection strengths while the anti-Hebbian plasticity depresses  
167 them in response to a stimulus.

168 The advantage of these learning rules is that they are built to reproduce patterns of  
169 activity observed in the PrC during familiarity, which correspond to physiological evidence  
170 (Brown & Aggleton, 2001; Brown & Xiang, 1998). In that way, models of that kind provide a  
171 biologically plausible implementation for familiarity recognition (Bogacz & Brown, 2003a;  
172 Bogacz et al., 2001b; Tyulmankov et al., 2022). Nevertheless, Hebbian and anti-Hebbian  
173 trainings seem to have distinct properties and thus operate differently from each other. For  
174 example, Bogacz & Brown (2003b) observed differences in performance whether inputs are  
175 correlated or not. More importantly, some authors argue that Hebbian learning is more  
176 biologically plausible than its anti-Hebbian counterpart. According to these authors, this is due  
177 to the fact that anti-Hebbian learning tries to reproduce synaptic mechanisms that they declare  
178 were not observed in the brain yet (Bogacz & Brown, 2003b). However, this lack of biological  
179 plausibility is still debated. In fact, recent works with meta-learning algorithms seems to be in

180 favor of anti-Hebbian models. In the model proposed by Tyulmankov et al. (2022), the network  
181 learns from itself (i.e., meta-learns) which one the two learning rules, that is the Hebbian or the  
182 anti-Hebbian, should be preferred during training. Authors showed that a network with meta-  
183 learning optimization is more likely to converge to the anti-Hebbian solution. Moreover, anti-  
184 Hebbian plasticity seems to generalize better and has a larger memory capacity than Hebbian  
185 plasticity (Tyulmankov et al., 2022). So, the question remains: which one of these learning rules  
186 should be preferred when one is trying to model familiarity using artificial neural networks?

187         The goal of this article is to understand, by means of computational models, the inner  
188 functioning of the Hebbian and anti-Hebbian training. By comparing how they operate, we want  
189 to explain differences in models' abilities on natural images. Therefore, we built two models  
190 respectively with Hebbian and anti-Hebbian type of learning rules. The models are preceded by  
191 a pre-trained CNN to extract features of images. In this article, we compared the two models'  
192 performance under two criteria. First, we replicated and administered Standing's behavioral  
193 experiment to the Hebbian and anti-Hebbian models. Standing's apparatus showed that  
194 familiarity has an almost unlimited capacity during a forced-choice recognition (FCR) task  
195 (Standing, 1973). This experiment is frequently used to test recognition models' performance.  
196 Secondly, we compared our models' performance during a FCR task regarding specific  
197 characteristics of the dataset.

## 198 METHODS

199         Model architectures and recognition task simulations were implemented with the Python  
200 3.9.11 software (<https://www.python.org/>, RRID:SCR\_008394). The code is available in open  
201 access on GitHub (<https://github.com/JRead98/master.git>, RRID:SCR\_002630). Note that for  
202 our modelling, we used basic model of artificial neurons and not spiking neurons.

## 203 **2.1. Model's architecture**

204 As our model was inspired by previous works, it therefore functions in a similar way  
205 (Ji-An et al., 2022; Kazanovich & Borisyuk, 2021). That is, it was designed as a two-step  
206 network combining deep learning and simple feedforward neural networks (see **Figure 1**). The  
207 goal of this architecture is to reproduce patterns of activity observed in the PrC leading to a  
208 familiarity decision during a recognition task.

209 **[Insert Figure 1]**

210 Training operates in two times. First, an image is presented to a pre-trained CNN – in  
211 this case ResNet50 – for feature extraction. This mimics the processing in the ventral pathway  
212 from visual associative areas to the PrC (Eichenbaum et al., 2007; Le Cun, 2019). This is the  
213 feature extraction module. Second, the output of the second-last layer of the CNN is used as an  
214 input for a memory module. The memory module is a simple two-layers feedforward network  
215 which will learn the features of an image thanks to an Hebbian or an anti-Hebbian learning rule  
216 (similar two-layers networks were also used in Androulidakis et al., 2008). The output of the  
217 memory module is used for familiarity discrimination during the testing phase.

## 218 **2.2. Feature extraction module**

219 We used a CNN called ResNet50 as our feature extraction module (He, Zhang, Ren, &  
220 Sun, 2015, 2016). More precisely, we used the version ResNet50 v1.5 which was previously  
221 trained on PyTorch with 1.2 million high-resolution photographs of natural images from  
222 ImageNet (Deng et al., 2009). ResNet50 was initialized as described in He et al. (2015).  
223 Originally, ResNet50 allows the classification of images in 1000 different categories with a  
224 high rate of accuracy. ResNet50 is built with 48 convolutional layers and 2 pooling layers to  
225 identify an image and define its characteristics according to different degrees of complexity.  
226 The penultimate layer of the model is a fully connected layer of 2048 features. We use this layer  
227 which corresponds to the embedding of the many successive convolutional layers to represent

228 the characteristics of an image. Note that in the complete architecture of ResNet50, the fully  
229 connected layer projects onto a SoftMax layer. This SoftMax allows the network to classify  
230 images. We do not use this last layer in our architecture.

231 Before going into the extraction module, the RGB representation of each images was  
232 normalized to the size 3x224x224 (as in Kazanovich & Borisyuk, 2021); 3 being the number of  
233 channels corresponding to the RGB colors and 224x224 the size of the images. For a given  
234 image, we retrieved a vector of 2048 features obtained at the penultimate fully connected layer  
235 of ResNet50. We consider this vector to represent the characteristics of this image. This vector  
236 is further used for image learning in the memory module. After passing through the CNN, the  
237 vector of size 2048 for a given image is collected then normalized. That is, the distribution of  
238 vector values has a mean of zero and a standard deviation of 1. We used this vector of real  
239 numbers as inputs for the memory module.

### 240 **2.3. Memory modules**

241 To reproduce familiarity decision, we implemented versions of the memory module that  
242 are similar to the version designed by Kazanovich & Borisyuk (2021). In contrast to Bogacz &  
243 Brown (2003b), we used simple neural networks instead of spiking neural networks.

244 Both Hebbian and anti-Hebbian modules are two-layers fully connected feedforward  
245 networks. Input layers consist of  $n = 2048$  neurons and output layers consist of  $m = 2048$  novelty  
246 neurons. Connection strengths (i.e., weights between inputs and outputs) are denoted  $w_{ij}$  and  
247 were initialized randomly between -1 and 1. The two learning rules differ in terms of weight  
248 modifications (**Figure 2**). Nevertheless, the formula to compute the activity in the output layer  
249 is the same for the Hebbian and anti-Hebbian model. That is, we used a forward propagation to  
250 compute the activity  $h_j$  of novelty neurons  $j$  according to the following formula:

$$251 \quad h_j = \sum_{i=1}^n w_{ij}x_i, \quad j = 1, \dots, n \quad (1)$$

252 where  $x_i$  is the vector of neurons activity for an image X after normalization in the feature  
253 extraction module and  $w_{ij}$  denotes the connection strengths.

254 Authors originally introduced the notion of active neurons as neurons whose number in  
255 the output layer must be limited (Bogacz et al., 2001; Bogacz & Brown, 2003a). We decided to  
256 reproduce this distinction between active neurons and neurons at rest using competition and  
257 inhibition (*k/2-winners*) as previously done in Androulidakis et al. (2008). More precisely, half  
258 of the novelty neurons with the highest activity are selected to be active (red circles in Figure  
259 2A). The other half are considered inactive and should not participate in the weight modification  
260 during the training phase (blue circles). We used the median of the overall activity to determine  
261 which neuron is active ( $>$  median) or inactive ( $\leq$  median). Active neurons took the value  $y_j = 1$   
262 and inactive neurons took the value  $y_j = 0$  (see **Figure 2A**).

263 **[Insert Figure 2]**

### 264 2.3.1. Hebbian learning rule

265 In the Hebbian learning rule, we assumed that the novelty neuron j is active only if the  
266 corresponding input neuron i is also active as previously done in Bogacz & Brown (2003b).  
267 Consequently, at the first presentation of an image X, the activity pattern of novelty neurons j  
268 ( $y$ ) is equal to the activity pattern of input neurons i ( $x$ ). Thus, in vector form, we consider that  
269 the initial response of the networks would be:

$$270 \quad x^X = y^X$$

271 where  $x^X$  is the vector of neurons activity for an image X after normalization in the  
272 feature extraction module and where  $y^X$  is the vector of novelty neurons activity for an image  
273 X. In the Hebbian model, we didn't use the activity of novelty neurons during training given  
274 this assumption that the initial response of the network is equal to the activity of input neurons.  
275 Instead, we started by applying the *k/2-winners* rule on the vector  $x^X$  to obtain the vector  $y^X$

276 constituted of 0s and 1s. We then applied the following weight modification formula (one  
277 should note that weights are not bounded and could thus be subject to saturation):

$$278 \quad w_{ij} = w_{ij} + \eta y_j x_i \quad (2)$$

279 where  $\eta = 0.01$  is the learning rate (this value has been found as the global minimum in  
280 Kazanovich & Borisyuk, 2021),  $x_i$  corresponds to the input neurons after normalization and  $y_j$   
281 corresponds to the input neurons after inhibition and competition. If  $y_j$  and  $x_i$  represent features  
282 of the input, then the learning rule will amplify the  $w_{ij}$  link between features that appear  
283 together. Here, learning occurs through the increase in connections strengths between co-  
284 occurring features as if by Long-Term Potentiation (Bliss & Collingridge, 1993). This weight  
285 modification is implemented a single time for each image of the training set. It will lead to an  
286 overall higher activity in the output layer when a familiar stimulus is presented again.

287 However, to correctly mimic the pattern of neuronal firing in the PrC during the  
288 presentation of a familiar stimulus, the activity of novelty neurons should be lower for familiar  
289 stimuli than novel ones (Brown & Aggleton, 2001; Brown & Xiang, 1998). To overcome this  
290 problem, the Hebbian model originally described by Bogacz et al. (2001) used an inhibitory  
291 interneuron to model the familiarity decision in the PrC. This inhibitory interneuron is  
292 computed from the activity of novelty neurons. It will represent the level of inhibition that  
293 should be used to reduce the activity of novelty neurons when a familiar stimulus is presented  
294 again. They argued that familiarity decision in their model could be implemented with two  
295 options (Bogacz et al., 2001; Bogacz et Brown, 2003b). First, with the reduced activity of the  
296 novelty neurons after inhibition by the inhibitory interneurons. Second, with the level of  
297 inhibition itself which should therefore be higher for familiar stimuli than for novel ones. Here,  
298 we decided to implement the second option during the testing phase. We used the activity of  
299 the output layer to compute an inhibition level  $d(X)$  as:

$$300 \quad d(X) = \sum_{j=1}^m x_j h_j \quad (3)$$

301 where  $h_j$  are the components from the vector of the novelty neurons computed with  
 302 formula (1) and  $x_j$  are the components from the vector of inputs neurons after normalization.  
 303 Familiar images should present a higher level of inhibition compared to novel images. Thus,  
 304 during a recognition task where a pair of images ( $X, Z$ ) is presented to the model, where  $X$  is an  
 305 old and  $Z$  is a novel image, a correct familiarity decision is made by the model if  $d(X) > d(Z)$ .  
 306 This can be easily seen by presenting the same image several times to the model during training.  
 307 This will amplify the  $w_{ij}$  links between active features, increasing  $h_j$  and consequently  
 308 increasing  $d(X)$  compared to a novel image  $d(Z)$ .

### 309 2.3.2. Anti-Hebbian learning rule

310 In the anti-Hebbian learning rule, on the opposite of the Hebbian learning rule, we  
 311 started by computing the activity  $h_j$  of the novelty neurons with formula (1) before applying the  
 312 weight modification formula. Thus, there was a diffusion of activity before the weight were  
 313 modified. Once the output layer is computed, we applied the *k/2-winner* rule on the components  
 314  $h_j$  to obtain  $y_j$ .

315 Here, learning occurs through the decrease in connections strengths between input  
 316 neurons and active novelty neurons as if by Long-Term Depression (Androulidakis et al., 2008;  
 317 Bogacz & Brown, 2003a; Ito, 1989). Therefore, weights are modified during training with the  
 318 following formula:

$$319 \quad w_{ij} = w_{ij} - \eta x_i y_j \quad (4)$$

320 where  $\eta = 0.01$  denotes the learning rate,  $x_i$  corresponds to the input neurons after  
 321 normalization and  $y_j$  corresponds to the components of the vector of novelty neurons after the  
 322 *k/2-winner* rule. This weight modification will slightly reduce the variance inside the vector of  
 323 novelty neurons  $h_j$  when computed again with formula (1). As in the Hebbian solution, this

324 weight modification is only implemented a single time for each image of the training set.  
325 Nevertheless, the variance reduction can be easily objectified if we repeatedly present a sole  
326 stimulus to the anti-Hebbian model. Indeed, after several presentations, the differences between  
327 values of novelty neurons for a given image will gradually decrease.

328 After each image has been studied by the model, we fix the connection strengths before  
329 the testing phase. Overall, we should observe an average activity in the output layer that is lower  
330 when a familiar stimulus is presented compared to a novel one. During the testing phase, we  
331 computed the average output activity to model the familiarity decision as in the Hebbian model  
332 with the following formula (Kazanovich & Borisyuk, 2021):

$$333 \quad d(X) = \frac{1}{m} (\sum_{j \in M1} h_j - \sum_{j \in M2} h_j) \quad (5)$$

334 where  $h_j$  are the components from the vector of the novelty neurons computed with  
335 formula (1) and M1 and M2 are respectively the sets of  $k/2$ -winners (active neurons) and -losers  
336 (inactive neurons) in the output layer. Familiar images should produce lower activity than novel  
337 images (Bogacz & Brown, 2003a). Indeed, if we present several times the same image to the  
338 network, the  $w_{ij}$  links will decrease, reducing  $h_j$  and consequently decreasing  $d(X)$ . Thus, during  
339 a recognition task where a pair of images ( $X, Z$ ) is presented to the model, where X is an old  
340 and Z is a novel image, a correct familiarity decision is made if  $d(X) < d(Z)$ .

## 341 **2.4. Simulation methodology**

342 The simulation methodology is depicted in **Figure 3** and was similar to that of  
343 Kazanovich & Borisyuk (2021). The methodological pipeline is identical for every simulation  
344 with a training phase followed by a testing phase. During the training phase, a model was trained  
345 on a subsample constituted of  $N$  images randomly taken from the corresponding dataset. Images  
346 were learned one-by-one with the weight modification specific to the selected memory module.  
347 Each image was presented once to the model for learning. In the testing phase, we implemented



348 a forced-choice recognition (FCR) task. During the FCR task,  $N$  pairs of images were presented  
349 simultaneously to the network: a new image as well as an image previously learned during  
350 training. The model had thus to decide which image is familiar depending on the memory  
351 module. If the model has chosen the new image as familiar, a recognition error was logged.

352 **[Insert Figure 3]**

## 353 RESULTS

354 All the plots were generated by using ggplot2 package (Wickham, 2009, [https://cran.r-](https://cran.r-project.org/web/packages/ggplot2/index.html)  
355 [project.org/web/packages/ggplot2/index.html](https://cran.r-project.org/web/packages/ggplot2/index.html), RRID:SCR\_014601). The data obtained during  
356 the different simulations and the script used to visualize them are openly available on the OSF  
357 platform (<https://osf.io/vpgdm/>, RRID:SCR\_003238).

358 As a first simulation, we reproduced Standing’s experiment to evaluate the memory  
359 capacity of the models with the methodological pipeline depicted in **Figure 3** (Standing, 1973).  
360 The dataset consisted of a database of about 30 000 natural images divided into 256 object  
361 categories (Caltech 256 Image Dataset; Griffin, Holub, & Perona, 2007). All categories  
362 contained in average 119 images and a minimum of 80 images.

363 As part of the simulation, we estimated the error probability ( $P_{err}$ ) for the entire task  
364 then averaged it on 100 runs of the models. Each run was realized with a different training and  
365 testing set. We also computed the number of images retained in memory, similarly to  
366 Kazanovich & Borisyuk (2021):

$$367 N_{ret} = N(1 - 2P_{err}) \quad (6)$$

368 where  $N$  is the number of images presented during training and  $P_{err}$  is the error  
369 probability for the entire task. Results from the first simulation are shown in **Figure 4**.

370 **[Insert Figure 4]**

371 As expected, we observed for both our models that performance decreases gradually as  
372 the dataset size increases (**Figure 4B**). That is, the error probability is on average worse when  
373 the models are tested with large datasets than with small datasets (**Table 1**). In the medium  
374 dataset size condition ( $N = 100$ ), both models still have good accuracy. However, when this  
375 threshold is crossed, the performance of the Hebbian model started to decrease more drastically  
376 than its anti-Hebbian counterpart.

377 In comparison with human data, we can see that anti-Hebbian model outperformed  
378 human performance until 1000 images are presented. As a matter of fact, it is only for the two  
379 biggest datasets ( $N = 4000$  and  $N = 10000$ ) that the anti-Hebbian model performs worse than  
380 human. One should note that the performance still reaches more than 65% accuracy with the  
381 highest dataset size, suggesting that the model didn't perform at chance level even in this  
382 condition. Regarding the Hebbian model, the probability of error is similar to human behavioral  
383 performance up to 40 images. Passed this dataset size, performance of the Hebbian model  
384 gradually decreased to reach random choices between familiar and novel images for the highest  
385 dataset size ( $P_{err} = 0.5$ ). This random choice pattern of answers tends to come up when more  
386 than 1000 images were presented during the training phase.

387 Moreover, we observed that the memory capacity for the anti-Hebbian solution is  
388 strikingly similar to human performance with on average  $\mu = 3-171.760$  ( $\sigma = 101.402$ ) images  
389 retained in memory for  $N = 10\ 000$ . In fact, it managed to have near perfect memory for most  
390 of the dataset sizes (**Table 1**). Overall, it tends to fit the power law observed in Standing's  
391 original experiment (**Figure 4A**). In comparison, the Hebbian solution seems to have a poor  
392 memory capacity which didn't exceed 376 images when 10 000 pictures are learned during  
393 training ( $\mu = 150.760$ ;  $\sigma = 90.912$ ). On average, the number of images retained in memory by  
394 the Hebbian model seems to be constant for every dataset size that exceeds a hundred pictures.

395

[Insert Table 1]

396 Next, we wanted to check whether the models could display a recency effect. To  
397 highlight such an effect, we estimated the probability that a network will make an error for a  
398 given pair of images during the testing phase and averaged it over 100 runs of the models. We  
399 performed the simulations at the threshold where models' performance started to diverge while  
400 they both kept more than 80% accuracy ( $N = 100$ ). Graphically, a recency effect should be  
401 marked by a gradual decrease in the average error probability as a function of the image position  
402 in the training phase. Results were then smoothed with a Loess Regression function and plotted  
403 in **Figure 5**.

404 **[Insert Figure 5]**

405 Interestingly, it seems that the anti-Hebbian model exhibits a recency effect that is not  
406 observed with the Hebbian model. The former has indeed lower probabilities of error for images  
407 learned at the end of the training (i.e., recent images) compared to images learned at the  
408 beginning of the training. This is not the case for the Hebbian model which showed no tendency  
409 to make less mistakes for recent images.

410 For the second simulation, we decided to test whether the models are sensitive to  
411 homogeneity between the inputs. We tested the performance of the models in three conditions  
412 of homogeneity: heterogeneity, mild homogeneity, high homogeneity. The heterogeneity  
413 condition consisted of random pictures selected from the Caltech 256 database (Griffin et al.,  
414 2007). The two homogeneous conditions consisted of two datasets, each constituted with only  
415 one semantic category of images, respectively dogs and cats. The mild homogeneity condition  
416 thus corresponded exclusively to dogs' pictures randomly selected for the dog's category folder  
417 from the Caltech 256 database (Griffin et al., 2007). Regarding the high homogeneity condition,  
418 we used exclusively cats' pictures randomly selected from the so-called "Cat Dataset", which  
419 consists of nearly 10 000 pictures of cats divided in 7 sub-folders (W. Zhang, Sun, & Tang,  
420 2008). We justify our choices on the fact the dogs have a wider variety of perceptual features

421 than cats (i.e. dogs are more heterogeneous than cats, French, Quinn, & Mareschal, 2001;  
422 Mareschal, French, & Quinn, 2000).

423 Simulations took place similarly as in the first simulation (see **Figure 3**). The only  
424 difference is that for the mild and high homogeneity conditions, models were trained  
425 exclusively with dogs or cats' pictures, respectively. For example, in the high homogeneity  
426 condition, models had to learn 40 images of cats ( $N = 40$ ). During the testing phase,  $N$  pairs of  
427 cats' pictures were presented to the model: a new and an old cat. The models had to decide  
428 which one was familiar.

429 As previously done, the results were average over 100 runs of the models. Each run was  
430 realized with a different training and testing set. The average  $P_{err}$  and standard deviations for  
431 the three homogeneity conditions are plotted in **Figure 6**.

432 **[Insert Figure 6]**

433 Foremost, the anti-Hebbian model has a better accuracy than the Hebbian model in every  
434 homogeneity condition. With the anti-Hebbian learning rule, model performance still reaches  
435 high accuracy in the high homogeneity condition. Performance is furthermore stable for the  
436 heterogeneity to the mild homogeneity, and we observed no decrease in accuracy between the  
437 two conditions. In fact, the anti-Hebbian model has a near perfect accuracy when trained and  
438 tested with low and no homogeneity between the inputs. With the Hebbian learning rule, we  
439 observed a gradual decrease as the homogeneity between the pictures increases during the  
440 learning phase. Moreover, we can see that when the Hebbian model is trained with cat pictures  
441 only (i.e., high homogeneity), the model responds randomly during the FCR task.

442 **[Insert Table 2]**

443 A summary of our key results is detailed in **Table 2**. For each simulation, we estimated  
444 the error probability ( $P_{err}$ ) for the entire task then averaged it on 100 runs of the models. Each

445 run was realized with a different training and testing set. We can observe that both the Hebbian  
446 and anti-Hebbian model have more than 80% accuracy on small, medium, and mildly  
447 homogeneous datasets. Besides, the accuracy is numerically higher in the anti-Hebbian model  
448 in every conditions. Regarding the performance of the Hebbian model on large and highly  
449 homogeneous dataset, it seems that the model failed 1 out of 2 times to correctly choose the  
450 familiar image. We interpreted these results as random answers.

## 451 DISCUSSION

452         The goal of the paper is to compare two learning rules which can be used to model  
453 familiarity by reproducing the pattern of neural firing observed in the PrC. Here, by  
454 differentiating Hebbian and anti-Hebbian learning on natural images, we want to provide  
455 insight into the operations at hands when a stimulus becomes familiar. We showed that the anti-  
456 Hebbian solution has on average a higher memory capacity than the Hebbian solution. Besides,  
457 the former fits relatively well Standing’s behavioral data (Standing, 1973) whereas the later  
458 only fits the data when the training set doesn’t exceed 40 images. Regarding their ability to  
459 manage homogeneity between the inputs, we showed that the anti-Hebbian model once again  
460 has better accuracy than its Hebbian counterpart. In fact, the anti-Hebbian model still reaches  
461 high accuracy even with highly homogeneous stimuli (i.e., cats). The Hebbian model reaches  
462 more than 80% accuracy in the mild homogeneity condition (i.e., dogs). Nevertheless, it fails  
463 to perform above chance in the high homogeneity condition suggesting high vulnerability to  
464 homogeneity.

465         On one hand, our results with the anti-Hebbian model are in line with previous networks  
466 using anti-Hebbian learning to model familiarity (Androulidakis et al., 2008; Kazanovich &  
467 Borisyyuk, 2021). Interestingly, in the model proposed by Kazanovich & Borisyyuk (2021), they  
468 did not implement inhibition and competition *per se*. Rather, they only applied formula (5) to

469 withdraw the activity from the sets of losers (i.e., half of the neurons in the output layer with  
470 the lowest activity) for the pair of images presented during the FRC task. Besides, they used  
471 AlexNet for features extraction instead of ResNet50 as in our modeling (Krizhevsky, Sutskever,  
472 & Hinton, 2012). Despite these slightly different implementations of the anti-Hebbian model,  
473 we still managed to reproduce their results on Standing’s experiment.

474         In addition, our results showed that the anti-Hebbian model can react to the more recent  
475 (i.e., familiar) stimuli with greater accuracy. More importantly, by reducing the overall activity  
476 in the output layer, it successfully reproduces the repetition suppression mechanisms observed  
477 in the brain when a stimulus becomes familiar (Grill-Spector et al., 2006; Meyer & Rust, 2018).  
478 According to Tanaka, Saito, Fukada, & Moriya (1991), repetition suppression is thought to be  
479 very selective for complex visual stimuli. In fact, it provides the specific information that would  
480 permit recognizing a recent stimulus. Taken together, this suggests that it is the anti-Hebbian  
481 learning rule ability to reduce the variance of the vector of novelty neurons that allows it to  
482 accurately model familiarity recognition (Bogacz & Brown, 2003a). If the target has lower  
483 variance in its output layer than the lure, it should mean that the target has more recency – or  
484 familiarity – than the lure. Our simulations showed that this ability is impaired neither by the  
485 number of presented stimuli nor by the similarity between targets lures.

486         On the other hand, to our knowledge, this is the first time that an Hebbian learning rule  
487 was implemented on natural images instead of artificial inputs. This makes the comparison with  
488 other networks difficult. Nevertheless, Bogacz & Brown (2003b) have previously shown that  
489 its performance should be lower than an anti-Hebbian model when there were dependances  
490 between the stimuli features. To address this issue, Kazanovich & Borisyuk (2021) have  
491 computed this dependances for the images from the Caltech 256 database. As expected, they  
492 showed that the co-occurrence between pairs of features could be high for some pictures. It is  
493 then plausible that differences in models’ performance to reproduce behavioral data could be

494 explained to some extent by co-occurrence between the features of an image. This is also in line  
495 with our results showing high sensitivity to homogeneity between inputs in the Hebbian model  
496 only. However, this raises the question: can the Hebbian solution provide an accurate modeling  
497 framework for familiarity recognition in human?

498         Based on the results of our simulations, we can reasonably admit that the Hebbian model  
499 can successfully discriminate between old and new pictures under certain conditions (small to  
500 medium dataset set, mild homogeneity in the training data). We also showed that our version  
501 of the Hebbian learning rules operates by encoding co-occurrence between features that  
502 appeared together in an image. This means that the learning rule will increase the connection  
503 strength between two active features of an input. For example, consider a picture of an old man  
504 as the stimulus. He has glasses, a beard, and a baldness that are considered as active features.  
505 The Hebbian model will increase the link between the glasses and the beard, between the  
506 baldness and the beard, and so on. In other words, the Hebbian model will create a global  
507 representation of a stimulus. This means, regarding recognition, that stimuli where glasses  
508 appear with beard and where baldness appears with glasses will be more familiar to the system.

509         Interestingly, this description of our Hebbian model is consistent with the global  
510 matching models (GMM) of recognition (Clark & Gronlund, 1996; Osth & Dennis, 2020). The  
511 assumption behind GMM is that an item is constituted of several memory representations (i.e.,  
512 several features). During a recognition task, a cued item will activate these representations. The  
513 activation of these components of an item will be combined to produce global match. If the  
514 match signal is high enough, it will lead to a familiarity judgment. More importantly, GMM  
515 predicts that high number of stimuli and similarity between stimuli (i.e., homogeneity) will both  
516 lead to impaired recognition judgment (M. Brandt, Zaiser, & Schnuerch, 2019; Cary, 2003).  
517 Along with the results from our simulations, this suggest that the Hebbian model could indeed  
518 correspond to a mechanism for familiarity recognition.

519           It has long been thought that familiarity could involve different co-existing mechanisms  
520 (Bastin et al., 2019; Mandler, 1980; Mecklinger & Bader, 2020). Therefore, the Hebbian and  
521 anti-Hebbian model should not be mutually exclusive. Instead, we believe that our models are  
522 quite complementary and can provide insight into answering questions of that sort. In a review  
523 article, Mecklinger & Bader (2020) highlight the distinction between an absolute familiarity  
524 and a relative familiarity. The former would be linked to stimuli that have been frequently  
525 encountered in our lifetime whereas the latter would be associated with stimuli that have been  
526 recently encountered (Bridger, Bader, & Mecklinger, 2014). More importantly, it has been  
527 shown that the PrC exhibits different patterns of activity in association with both absolute and  
528 relative familiarity (Daselaar, Fleck, & Cabeza, 2006; Diana, Yonelinas, & Ranganath, 2007;  
529 Duke, Martin, Bowles, McRae, & Köhler, 2017). Along with the work of Xiang & Brown  
530 (1998) on monkeys, it has been suggested that the reduced firing pattern (i.e., repetition  
531 suppression) observed in some neurons of the PrC would be associated with relative familiarity.  
532 It would result in a decrease in the signal strength, similarly to what we observed in our anti-  
533 Hebbian model. On the other hand, other PrC neurons have shown a selective firing pattern to  
534 stimuli with high absolute familiarity. In agreement with our Hebbian model, absolute  
535 familiarity would induce an increase in the signal strength as measured by  $d(X)$  (Mecklinger &  
536 Bader, 2020; Xiang & Brown, 1998).

537           For now, we don't know precisely how these two familiarity processes are articulated  
538 together. Coane, Balota, Dolan, & Jacoby (2011) tried to answer this question by clarifying the  
539 time course of the familiarity signal. Previous works showed that items already have a baseline  
540 familiarity whose level depends on how often an item has been encountered during the lifespan  
541 (Joordens & Hockley, 2000; Reder et al., 2000). Coane et al. (2011) hypothesized that when an  
542 item is studied, it acquires a temporary increase in its familiarity signal in addition to a  
543 permanent increase in its absolute level of familiarity (**Figure 7A**). This temporary familiarity



544 boost corresponds to the relative level of familiarity. Unfortunately, this framework does not  
545 tell us about the conditions for a mechanism to take precedence over another.

546 Our modeling framework allows us to make the following predictions by separating the  
547 contribution of absolute and relative familiarity to the phenomenological feeling of familiarity  
548 (**Figure 7B**). Here, we first assume that the Hebbian learning rule models exclusively absolute  
549 familiarity through the overall structure of the stimulus, like in GMM. On the opposite, the anti-  
550 Hebbian learning rule models exclusively the relative familiarity through the recency of a  
551 stimulus. At first, both mechanisms could participate in familiarity decisions when the  
552 distinctiveness between stimuli is high. However, when the number of stimuli learned increases,  
553 absolute familiarity alone would not be efficient anymore as shown by the green line in **Figure**  
554 **7B** (M. Brandt et al., 2019; Cary, 2003). That is because stimuli become more and more  
555 homogeneous. In turn, more homogeneity – meaning less distinctiveness between the stimuli –  
556 increases the response criterion necessary to make familiarity judgments. In these conditions,  
557 we could only rely on relative familiarity mechanism to maintain recognition accuracy, as  
558 shown by the blue line.

559 Overall, our framework allows us to make testable predictions. More precisely, the  
560 advanced hypothesis could be further explored in patients at risk of Alzheimer's disease as the  
561 PrC is one of the first regions affected by the disease (Braak, Thal, Ghebremedhin, & Del  
562 Tredici, 2011). Interestingly, this population showed a selective relative familiarity impairment,  
563 with preserved absolute familiarity (Anderson, Baena, Yang, & Köhler, 2021). With the aim of  
564 disentangling the respective contributions of relative and absolute familiarity in Alzheimer's  
565 patients, one could easily imagine a recognition task administered in different homogeneity  
566 conditions such as in our second simulation (see Delhaye, Folville, & Bastin, 2019, for an  
567 example of paradigm). The prediction would be that Alzheimer's patients should exhibit  
568 impaired relative familiarity responses regardless of the homogeneity condition. In contrast,

569 they should exhibit preserved absolute familiarity responses only in low homogeneity  
570 conditions.

571         As expected, our study has several limitations that should be acknowledged. To begin  
572 with, we wanted to highlight the influence of the CNN on our results. Indeed, it is plausible that  
573 the reason why our Hebbian model is highly sensitive to homogeneity is due to the way features  
574 are extracted by ResNet50. ResNet50 – as most of other CNN – was trained to categorize  
575 pictures (He et al., 2016; Krizhevsky et al., 2012); i.e., this picture is a dog, this picture is a cat.  
576 That is what a CNN is trained to do but its inner mechanism is still a black box. Thus, in our  
577 models, the vector of 2048 features extracted from the second-last layer of the network has been  
578 designed during the training to represent the concept of cat. If we present a picture of another  
579 cat to the CNN, the new vector of features could be highly similar to the last picture categorized  
580 as a cat by ResNet50. Put in other words, it is plausible that our CNN does not extract the  
581 feature of the image *per se* but rather the features of the concept of “cat” itself. This would  
582 explain why it is more difficult to choose correctly between two similar images as in our second  
583 simulation. However, the lack of similarity effect on the ability of the anti-Hebbian model lets  
584 us think that our CNN does not impact that much the results from our simulations.

585         Another limitation is linked to our reproduction of the initial Hebbian model of Bogacz  
586 et al. (2001b). Indeed, in their original paper, they used an inhibitory interneuron to reduce the  
587 activity in the output layer after a stimulus is presented for the first time. This is to adequately  
588 reproduce the functioning of the PrC. By ease of computation, we decided not to implement  
589 this downsize of activity (Bogacz & Brown, 2003b). Rather, we directly used the so-called level  
590 of inhibition - which should be used to reproduce repetition suppression – in our decision  
591 function. One could therefore say that our model is incomplete in comparison to the model of  
592 Bogacz et al. (2001b). It would therefore be interesting to enhance our Hebbian model to see if  
593 our arbitrary simplification could have a profound impact on its performance.

594 Finally, it seems apparent that both models are too simple to account for the whole  
595 diversity of a phenomenon such as familiarity. For example, artificial neural networks as used  
596 in our works don't even consider the temporal dimension of synaptic plasticity (L. I. Zhang,  
597 Tao, Holt, Harris, & Poo, 1998). One way to overcome this problem would be to use spiking  
598 neural networks such as in other computational models of recognition (Ji-An et al., 2022;  
599 Norman & O'Reilly, 2003). Moreover, we do not implement the contribution of other brain  
600 area which are known to take part during familiarity (Bastin et al., 2019). As an example, it has  
601 been shown that the anterolateral entorhinal cortex is associated with familiarity recognition on  
602 images with overlapping features (Besson, Simon, Salmon, & Bastin, 2020). Thus, the  
603 integration of other part of the transentorhinal cortex in our modelling framework could be a  
604 promising way to capture more adequately the functioning of familiarity mechanisms (Bastin  
605 & Delhay, 2023; Besson et al., 2020).

## 606 CONCLUSION

607 In conclusion, we designed two computational models of familiarity in the PrC, the anti-  
608 Hebbian and the Hebbian models. We argued that these models should be viewed as  
609 complementary as they account for two distinct familiarity mechanisms, respectively relative  
610 and absolute familiarity. On one hand, the anti-Hebbian model reduces the variance inside the  
611 output layer to compute the recency of an item, which would be a suitable mechanism for  
612 relative familiarity. On the other hand, the Hebbian model increases the link between co-  
613 occurring features to produce a global match between features activation and a cued item, which  
614 would in turn be related to absolute familiarity. We also hypothesized that the contributions of  
615 these familiarity processes to recognition can be dissociated when there is not enough  
616 distinctiveness between items. To extent this framework, we could challenge predictions made  
617 by the models with experimental studies on real subjects.

618 **REFERENCES**

- 619 Aggleton, J. P., & Brown, M. W. (2006). Interleaving brain systems for episodic and  
620 recognition memory. *Trends in Cognitive Sciences*, *10*(10), 455–463.  
621 <https://doi.org/10.1016/j.tics.2006.08.003>
- 622 Anderson, N. D., Baena, E., Yang, H., & Köhler, S. (2021). Deficits in recent but not lifetime  
623 familiarity in amnesic mild cognitive impairment. *Neuropsychologia*, *151*, 107735.  
624 <https://doi.org/10.1016/j.neuropsychologia.2020.107735>
- 625 Androulidakis, Z., Lulham, A., Bogacz, R., & Brown, M. W. (2008). Computational models  
626 can replicate the capacity of human recognition memory. *Network: Computation in*  
627 *Neural Systems*, *19*(3), 161–182. <https://doi.org/10.1080/09548980802412638>
- 628 Bastin, C., Besson, G., Simon, J., Delhaye, E., Geurten, M., Willems, S., & Salmon, E. (2019).  
629 An Integrative Memory model of recollection and familiarity to understand memory  
630 deficits. *Behavioral and Brain Sciences*. <https://doi.org/10.1017/S0140525X19000621>
- 631 Bastin, C., & Delhaye, E. (2023). Targeting the function of the transentorhinal cortex to identify  
632 early cognitive markers of Alzheimer’s disease. *Cognitive, Affective, & Behavioral*  
633 *Neuroscience*. <https://doi.org/10.3758/s13415-023-01093-5>
- 634 Besson, G., Ceccaldi, M., & Barbeau, E. J. (2012). L’évaluation des processus de la mémoire  
635 de reconnaissance. *Rev Neuropsychol*, *4*(4), 242–254.  
636 <https://doi.org/10.1684/nrp.2012.0238>
- 637 Besson, G., Simon, J., Salmon, E., & Bastin, C. (2020). Familiarity for entities as a sensitive  
638 marker of antero-lateral entorhinal atrophy in amnesic mild cognitive impairment.  
639 *Cortex*, *128*, 61–72. <https://doi.org/10.1016/j.cortex.2020.02.022>
- 640 Bliss, T. V. P., & Collingridge, G. L. (1993). A synaptic model of memory: Long-term  
641 potentiation in the hippocampus. *Nature*, *361*(6407), 31–39.  
642 <https://doi.org/10.1038/361031a0>

643 Bogacz, R., & Brown, M. W. (2003a). An anti-Hebbian model of familiarity discrimination in  
644 the perirhinal cortex. *Neurocomputing*, *52*, 1–6. [https://doi.org/10.1016/s0925-](https://doi.org/10.1016/s0925-2312(02)00738-5)  
645 [2312\(02\)00738-5](https://doi.org/10.1016/s0925-2312(02)00738-5)

646 Bogacz, R., & Brown, M. W. (2003b). Comparison of computational models of familiarity  
647 discrimination in the perirhinal cortex. *Hippocampus*, *13*(4), 494–524.  
648 <https://doi.org/10.1002/hipo.10093>

649 Bogacz, R., Brown, M. W., & Giraud-Carrier, C. (2001a). High Capacity Neural Networks for  
650 Familiarity Discrimination. *Journal of Computational Neuroscience*, *10*(1), 5–23.  
651 <https://doi.org/10.1023/A:1008925909305>

652 Bogacz, R., Brown, M. W., & Giraud-Carrier, C. (2001b). Model of Familiarity Discrimination  
653 in the Perirhinal Cortex. *Journal of Computational Neuroscience*, *10*, 5–23.

654 Bowles, B., Crupi, C., Pigott, S., Parrent, A., Wiebe, S., Janzen, L., & Köhler, S. (2010). Double  
655 dissociation of selective recollection and familiarity impairments following two  
656 different surgical treatments for temporal-lobe epilepsy. *Neuropsychologia*, *48*(9),  
657 2640–2647. <https://doi.org/10.1016/J.NEUROPSYCHOLOGIA.2010.05.010>

658 Braak, H., Thal, D. R., Ghebremedhin, E., & Del Tredici, K. (2011). Stages of the Pathologic  
659 Process in Alzheimer Disease: Age Categories From 1 to 100 Years. *Journal of*  
660 *Neuropathology & Experimental Neurology*, *70*(11), 960–969.  
661 <https://doi.org/10.1097/NEN.0b013e318232a379>

662 Brandt, K. R., Eysenck, M. W., Nielsen, M. K., & von Oertzen, T. J. (2016). Selective lesion  
663 to the entorhinal cortex leads to an impairment in familiarity but not recollection. *Brain*  
664 *and Cognition*, *104*, 82–92. <https://doi.org/10.1016/J.BANDC.2016.02.005>

665 Brandt, M., Zaiser, A.-K., & Schnuerch, M. (2019). Homogeneity of item material boosts the  
666 list length effect in recognition memory: A global matching perspective. *Journal of*

667 *Experimental Psychology: Learning, Memory, and Cognition*, 45(5), 834–850.  
668 <https://doi.org/10.1037/xlm0000594>

669 Bridger, E. K., Bader, R., & Mecklinger, A. (2014). More ways than one: ERPs reveal multiple  
670 familiarity signals in the word frequency mirror effect. *Neuropsychologia*, 57, 179–190.  
671 <https://doi.org/10.1016/j.neuropsychologia.2014.03.007>

672 Brown, M. W., & Aggleton, J. P. (2001). Recognition memory: What are the roles of the  
673 perirhinal cortex and hippocampus? *Nature Reviews Neuroscience*, 2(1), 51–61.  
674 <https://doi.org/10.1038/35049064>

675 Brown, M. W., & Xiang, J. Z. (1998). Recognition memory: Neuronal substrates of the  
676 judgement of prior occurrence. *Progress in Neurobiology*, 55(2), 149–189.  
677 [https://doi.org/10.1016/S0301-0082\(98\)00002-1](https://doi.org/10.1016/S0301-0082(98)00002-1)

678 Cary, M. (2003). A dual-process account of the list-length and strength-based mirror effects in  
679 recognition. *Journal of Memory and Language*, 49(2), 231–248.  
680 [https://doi.org/10.1016/S0749-596X\(03\)00061-5](https://doi.org/10.1016/S0749-596X(03)00061-5)

681 Clark, S. E., & Gronlund, S. D. (1996). Global matching models of recognition memory: How  
682 the models match the data. *Psychonomic Bulletin & Review*, 3(1), 37–60.  
683 <https://doi.org/10.3758/BF03210740>

684 Coane, J. H., Balota, D. A., Dolan, P. O., & Jacoby, L. L. (2011). Not all sources of familiarity  
685 are created equal: The case of word frequency and repetition in episodic recognition.  
686 *Memory & Cognition*, 39(5), 791–805. <https://doi.org/10.3758/s13421-010-0069-5>

687 Cowell, R. A. (2012). Computational models of perirhinal cortex function. *Hippocampus*,  
688 22(10), 1952–1964. <https://doi.org/10.1002/hipo.22064>

689 Daselaar, S. M., Fleck, M. S., & Cabeza, R. (2006). Triple Dissociation in the Medial Temporal  
690 Lobes: Recollection, Familiarity, and Novelty. *Journal of Neurophysiology*, 96(4),  
691 1902–1911. <https://doi.org/10.1152/jn.01029.2005>

692 Delhaye, E., Folville, A., & Bastin, C. (2019). How to induce an age-related benefit of semantic  
693 relatedness in associative memory: It's all in the design. *Psychology and Aging, 34*(4),  
694 572–586. <https://doi.org/10.1037/pag0000360>

695 Deng, J., Dong, W., Socher, R., Li, L.-J., Li, K., & Fei-Fei, L. (2009). ImageNet: A Large-Scale  
696 Hierarchical Image Database. *CVPR09*.

697 Diana, R. A., Reder, L. M., Arndt, J., & Park, H. (2006). Models of recognition: A review of  
698 arguments in favor of a dual-process account. *Psychonomic Bulletin & Review, 13*(1),  
699 1–21. <https://doi.org/10.3758/BF03193807>

700 Diana, R. A., Yonelinas, A. P., & Ranganath, C. (2007). Imaging recollection and familiarity  
701 in the medial temporal lobe: A three-component model. *Trends in Cognitive Sciences,*  
702 *11*(9), 379–386. <https://doi.org/10.1016/j.tics.2007.08.001>

703 Duke, D., Martin, C. B., Bowles, B., McRae, K., & Köhler, S. (2017). Perirhinal cortex tracks  
704 degree of recent as well as cumulative lifetime experience with object concepts. *Cortex,*  
705 *89*, 61–70. <https://doi.org/10.1016/j.cortex.2017.01.015>

706 Eichenbaum, H., Yonelinas, A. P., & Ranganath, C. (2007). The Medial Temporal Lobe and  
707 Recognition Memory. *Annual Review of Neuroscience, 30*(1), 123–152.  
708 <https://doi.org/10.1146/annurev.neuro.30.051606.094328>

709 French, R. M., Quinn, P. C., & Mareschal, D. (2001). Reversing Category Exclusivities in  
710 Infant Perceptual Categorization: Simulations and Data. *Proceedings of the Annual*  
711 *Meeting of the Cognitive Science Society, (23)*, 23.

712 Griffin, G., Holub, A. D., & Perona, P. (2007). *Caltech 256. Object category dataset: Caltech*  
713 *Technical Report*. <https://doi.org/www.kaggle.com/datasets/jessicali9530/caltech256>

714 Grill-Spector, K., Henson, R., & Martin, A. (2006). Repetition and the brain: Neural models of  
715 stimulus-specific effects. *Trends in Cognitive Sciences, 10*(1), 14–23.  
716 <https://doi.org/10.1016/J.TICS.2005.11.006>

717 He, K., Zhang, X., Ren, S., & Sun, J. (2015). Delving deep into rectifiers: Surpassing human-  
718 level performance on imagenet classification. *Proceedings of the IEEE International*  
719 *Conference on Computer Vision*, 1026–1034.

720 He, K., Zhang, X., Ren, S., & Sun, J. (2016). Deep residual learning for image recognition.  
721 *Proceedings of the IEEE Conference on Computer Vision and Pattern Recognition*,  
722 770–778.

723 Hebb, D. O. (1949). *The Organization of Behavior*. New York: Wiley.

724 Humphreys, G. W., & Riddoch, M. J. (2006). Features, objects, action: The cognitive  
725 neuropsychology of visual object processing, 1984–2004. *Cognitive Neuropsychology*,  
726 23(1), 156–183. <https://doi.org/10.1080/02643290542000030>

727 Ito, M. (1989). Long-Term Depression. *Annual Review of Neuroscience*, 12(1), 85–102.  
728 <https://doi.org/10.1146/annurev.ne.12.030189.000505>

729 Jacoby, L. L. (1991). A process dissociation framework: Separating automatic from intentional  
730 uses of memory. *Journal of Memory and Language*, 30(5), 513–541.  
731 [https://doi.org/10.1016/0749-596X\(91\)90025-F](https://doi.org/10.1016/0749-596X(91)90025-F)

732 Ji-An, L., Stefanini, F., Benna, M. K., & Fusi, S. (2022). Face familiarity detection with  
733 complex synapses. *BioRxiv*, 854059. <https://doi.org/10.1101/854059>

734 Joordens, S., & Hockley, W. E. (2000). Recollection and familiarity through the looking glass:  
735 When old does not mirror new. *Journal of Experimental Psychology: Learning,*  
736 *Memory, and Cognition*, 26(6), 1534–1555. [https://doi.org/10.1037/0278-](https://doi.org/10.1037/0278-7393.26.6.1534)  
737 [7393.26.6.1534](https://doi.org/10.1037/0278-7393.26.6.1534)

738 Kazanovich, Y., & Borisyuk, R. (2021). A computational model of familiarity detection for  
739 natural pictures, abstract images, and random patterns: Combination of deep learning  
740 and anti-Hebbian training. *Neural Networks*, 143, 628–637.  
741 <https://doi.org/10.1016/j.neunet.2021.07.022>



742 Krizhevsky, A., Sutskever, I., & Hinton, G. E. (2012). ImageNet Classification with Deep  
743 Convolutional Neural Networks. In F. Pereira, C. J. Burges, L. Bottou, & K. Q.  
744 Weinberger (Eds.), *Advances in Neural Information Processing Systems* (Vol. 25, pp.  
745 1097–1105). Curran Associates, Inc.

746 Le Cun, Y. (2019). *Quand la machine apprend: La révolution des neurones artificiels et de*  
747 *l'apprentissage profond*. Odile Jacob.

748 Mandler, G. (1980). Recognizing: The Judgment of Previous Occurrence. *Psychological*  
749 *Review*, 87(3), 252–271. <https://doi.org/10.1037/0033-295X.87.3.252>

750 Mareschal, D., French, R. M., & Quinn, P. C. (2000). A connectionist account of asymmetric  
751 category learning in early infancy. *Developmental Psychology*, 36(5), 635–645.  
752 <https://doi.org/10.1037/0012-1649.36.5.635>

753 McClelland, J. L., McNaughton, B. L., & O'Reilly, R. C. (1995). Why There Are  
754 Complementary Learning Systems in the Hippocampus and Neocortex: Insights From  
755 the Successes and Failures of Connectionist Models of Learning and Memory.  
756 *Psychological Review*, 102(3), 419–457. <https://doi.org/10.1037/0033-295X.102.3.419>

757 Mecklinger, A., & Bader, R. (2020). From fluency to recognition decisions: A broader view of  
758 familiarity-based remembering. *Neuropsychologia*, 146, 107527.  
759 <https://doi.org/10.1016/j.neuropsychologia.2020.107527>

760 Merkow, M. N., Burke, J. F., & Kahana, M. J. (2015). The human hippocampus contributes to  
761 both the recollection and familiarity components of recognition memory. *Proceedings*  
762 *of the National Academy of Sciences*, 112(46), 14378–14383.  
763 <https://doi.org/10.1073/pnas.1513145112>

764 Meyer, T., & Rust, N. C. (2018). *Single-exposure visual memory judgments are reflected in*  
765 *inferotemporal cortex*. <https://doi.org/10.7554/eLife.32259.001>

766 Montaldi, D., & Mayes, A. R. (2010). The role of recollection and familiarity in the functional  
767 differentiation of the medial temporal lobes. *Hippocampus*, 20(11), 1291–1314.  
768 <https://doi.org/10.1002/hipo.20853>

769 Norman, K. A. (2010). How hippocampus and cortex contribute to recognition memory:  
770 Revisiting the complementary learning systems model. *Hippocampus*, 20(11), 1217–  
771 1227. <https://doi.org/10.1002/hipo.20855>

772 Norman, K. A., & O'Reilly, R. C. (2003). Modeling Hippocampal and Neocortical  
773 Contributions to Recognition Memory: A Complementary-Learning-Systems  
774 Approach. *Psychological Review*, 110(4), 611–646. [https://doi.org/10.1037/0033-  
775 295X.110.4.611](https://doi.org/10.1037/0033-295X.110.4.611)

776 Osth, A. F., & Dennis, S. (2020). *Global matching models of recognition memory* [Preprint].  
777 PsyArXiv. <https://doi.org/10.31234/osf.io/mja6c>

778 Reder, L. M., Nhouyvanisvong, A., Schunn, C. D., Ayers, M. S., Angstadt, P., & Hiraki, K.  
779 (2000). A mechanistic account of the mirror effect for word frequency: A computational  
780 model of remember–know judgments in a continuous recognition paradigm. *Journal of*  
781 *Experimental Psychology: Learning, Memory, and Cognition*, 26(2), 294–320.  
782 <https://doi.org/10.1037/0278-7393.26.2.294>

783 Ritchey, M., Libby, L. A., & Ranganath, C. (2015). Cortico-hippocampal systems involved in  
784 memory and cognition. In *Progress in Brain Research* (Vol. 219, pp. 45–64). Elsevier.  
785 <https://doi.org/10.1016/bs.pbr.2015.04.001>

786 Scalici, F., Caltagirone, C., & Carlesimo, G. A. (2017). The contribution of different prefrontal  
787 cortex regions to recollection and familiarity: A review of fMRI data. *Neuroscience &*  
788 *Biobehavioral Reviews*, 83, 240–251.  
789 <https://doi.org/10.1016/J.NEUBIOREV.2017.10.017>

790 Sohal, V. S., & Hasselmo, M. E. (2000). A model for experience-dependent changes in the  
791 responses of inferotemporal neurons. *Network: Computation in Neural Systems*, *11*(3),  
792 169–190. [https://doi.org/10.1088/0954-898X\\_11\\_3\\_301](https://doi.org/10.1088/0954-898X_11_3_301)

793 Standing, L. (1973). Learning 10,000 pictures. *Quarterly Journal of Experimental Psychology*,  
794 *25*, 207–222. <https://doi.org/10.1080/14640747308400340>

795 Tanaka, K., Saito, H., Fukada, Y., & Moriya, M. (1991). Coding visual images of objects in the  
796 inferotemporal cortex of the macaque monkey. *Journal of Neurophysiology*, *66*(1), 170–  
797 189. <https://doi.org/10.1152/jn.1991.66.1.170>

798 Tulving, E. (1985). Memory and consciousness. *Canadian Psychology/Psychologie*  
799 *Canadienne*, *26*(1), 1. <https://doi.org/10.1037/h0080017>

800 Tyulmankov, D., Yang, G. R., & Abbott, L. F. (2022). Meta-learning synaptic plasticity and  
801 memory addressing for continual familiarity detection. *Neuron*, *110*(3), 544-557.e8.  
802 <https://doi.org/10.1016/j.neuron.2021.11.009>

803 Wickham, H. (2009). *ggplot2: Elegant Graphics for Data Analysis*. New York, NY: Springer  
804 New York. <https://doi.org/10.1007/978-0-387-98141-3>

805 Wolk, D. A., Dunfee, K. L., Dickerson, B. C., Aizenstein, H. J., & Dekosky, S. T. (2011). A  
806 Medial Temporal Lobe Division of Labor: Insights From Memory in Aging and Early  
807 Alzheimer Disease. *Hippocampus*, *21*(5), 461–466. <https://doi.org/10.1002/hipo.20779>

808 Xiang, J. Z., & Brown, M. W. (1998). Differential neuronal encoding of novelty, familiarity  
809 and recency in regions of the anterior temporal lobe. *Neuropharmacology*, *37*(4–5),  
810 657–676. [https://doi.org/10.1016/S0028-3908\(98\)00030-6](https://doi.org/10.1016/S0028-3908(98)00030-6)

811 Yonelinas, A. P. (2002). The nature of recollection and familiarity: A review of 30 years of  
812 research. *Journal of Memory and Language*, *46*(3), 441–517.  
813 <https://doi.org/10.1006/jmla.2002.2864>

814 Yonelinas, A. P., Aly, M., Wang, W. C., & Koen, J. D. (2010). Recollection and familiarity:  
815 Examining controversial assumptions and new directions. *Hippocampus*, *20*(11), 1178–  
816 1194. <https://doi.org/10.1002/hipo.20864>

817 Yonelinas, A. P., Otten, L. J., Shaw, K. N., & Rugg, M. D. (2005). Separating the Brain Regions  
818 Involved in Recollection and Familiarity in Recognition Memory. *The Journal of*  
819 *Neuroscience*, *25*(11), 3002–3008. <https://doi.org/10.1523/JNEUROSCI.5295-04.2005>

820 Yonelinas, A. P., Ramey, M. M., & Riddell, C. (2022). *Recognition Memory: The Role of*  
821 *Recollection and Familiarity*. Handbook of Human Memory: Foundations and  
822 Applications. Oxford University Press.

823 Zhang, L. I., Tao, H. W., Holt, C. E., Harris, W. A., & Poo, M. (1998). A critical window for  
824 cooperation and competition among developing retinotectal synapses. *Nature*,  
825 *395*(6697), 37–44. <https://doi.org/10.1038/25665>

826 Zhang, W., Sun, J., & Tang, X. (2008). Cat head detection-how to effectively exploit shape and  
827 texture features. *European Conference on Computer Vision*, 802–816. Springer.

828

829

830

831

832

833

834

835

836

837

838

**Table 1**

Number of images retained in memory ( $N_{ret}$ ) by the Hebbian and anti-Hebbian models for different dataset sizes.

<b>Anti-Hebbian</b>	<b>Dataset Size</b>							
	<b>20</b>	<b>40</b>	<b>100</b>	<b>200</b>	<b>400</b>	<b>1000</b>	<b>4000</b>	<b>10000</b>
Mean	20.00	39.860	97.90	189.680	357.70	744.720	1786.180	3171.760
Std. Deviation	0.00	0.586	2.418	4.720	10.661	22.256	63.583	101.402
Minimum	20.00	36.00	90.00	180.00	332.00	678.00	1632.00	2932.00
Maximum	20.00	40.00	100.00	200.00	378.00	798.00	1928.00	3564.00
<b>Hebbian</b>								
Mean	19.920	38.380	73.440	91.760	100.140	107.820	128.560	150.760
Std. Deviation	0.394	1.879	6.781	12.112	17.294	29.666	61.671	90.912
Minimum	18.00	32.00	52.00	60.00	52.00	50.00	12.00	0.00
Maximum	20.00	40.00	90.00	124.00	144.00	188.00	282.00	376.00

840

**Table 2**

Accuracy for the Hebbian and anti-Hebbian model computed during the testing phase in every dataset condition.

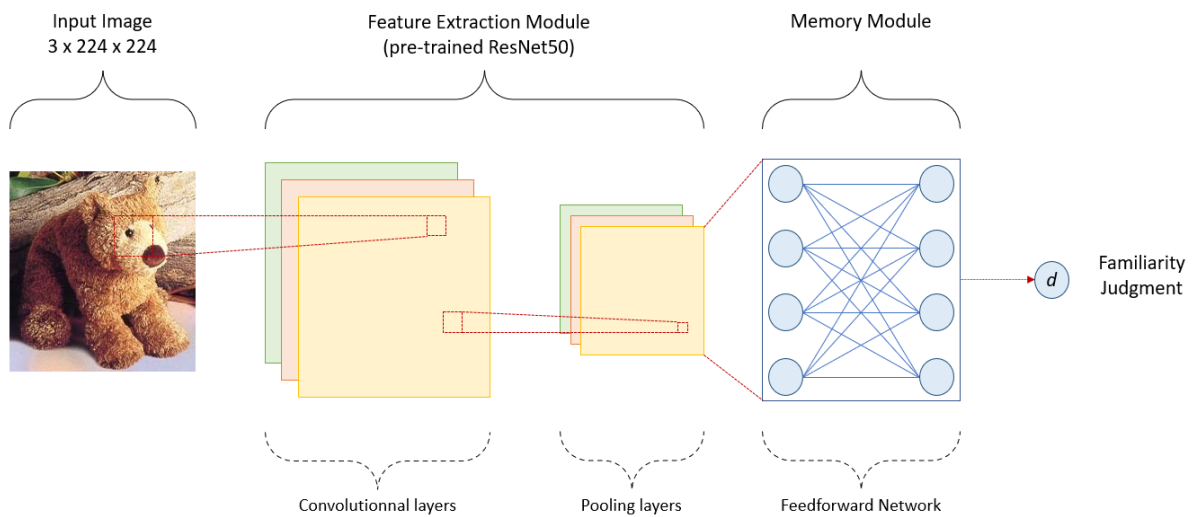
<b>Dataset Size</b>	<b>Model</b>	
	<b>Anti-Hebbian</b>	<b>Hebbian</b>
Small dataset (N = 20)	100.00 (0.00)	99.80 (1.00)
Medium dataset (N = 100)	98.90 (1.20)	86.70 (3.40)
Large dataset (N = 1000)	87.20 (1.10)	55.40 (01.50)
<b>Dataset Type (N = 40)</b>		
Heterogeneous (random)	99.80 (0.7)	98.00 (2.30)
Mild homogeneity (dogs)	99.90 (0.5)	82.90 (5.10)
High homogeneity (cats)	91.30 (4.50)	56.80 (7.50)

*Note.* Mean % over 100 runs (standard deviation).

841

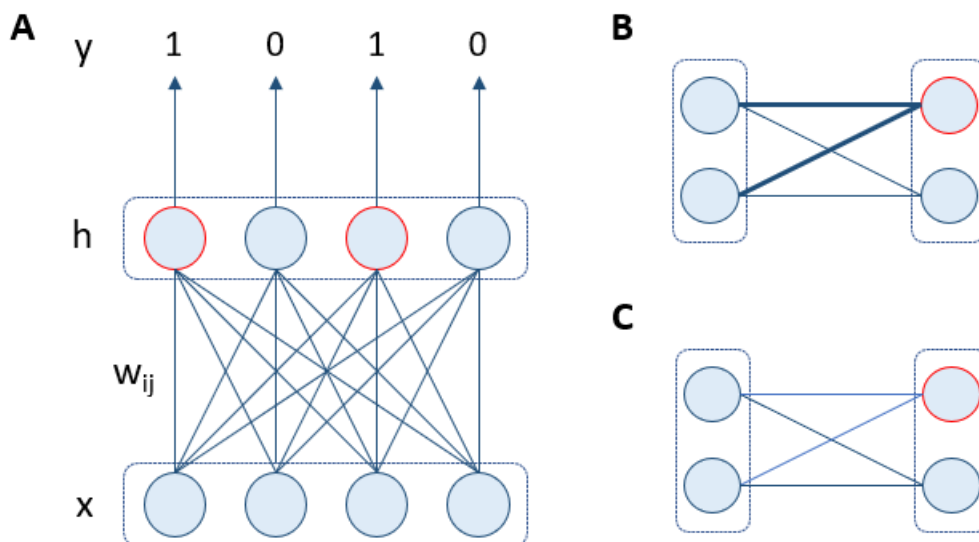
842 **FIGURE**

843 **Figure 1.** Global architecture of the models. An image goes through ResNet50 for features  
844 extraction then inside a memory module for learning. During the testing phase, a familiarity  
845 score  $d$  is computed for decision making.



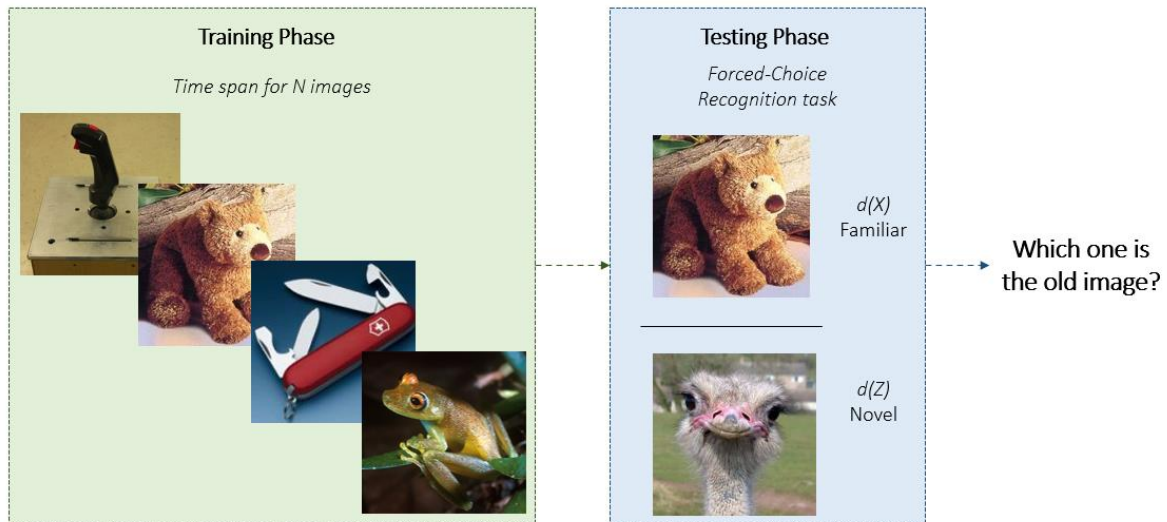
846

847 **Figure 2.** Learning rules inside the memory modules. (A) General idea behind the functioning  
848 of the memory module. (B) Weight potentiation for active neurons in the Hebbian model. (C)  
849 Weight depression for active neurons in the anti-Hebbian model.



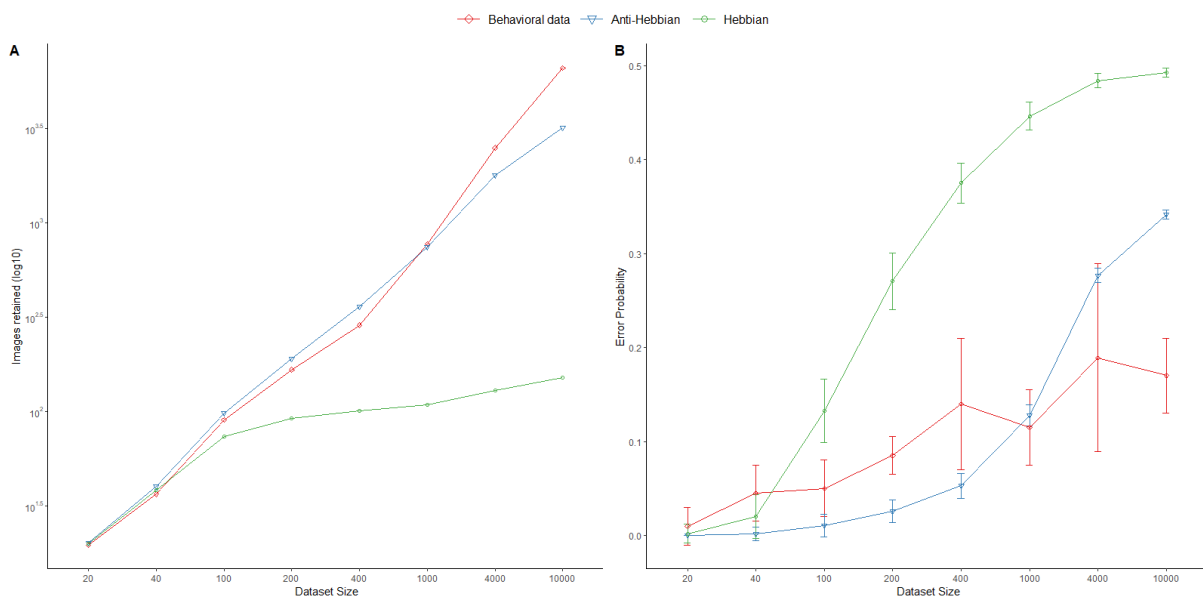
850

851 **Figure 3.** Simulation methodology. During the training phase,  $N$  images are learned one-by-  
 852 one by the model. During the testing phase, pairs of images are presented to the model which  
 853 has to decide which image is familiar.



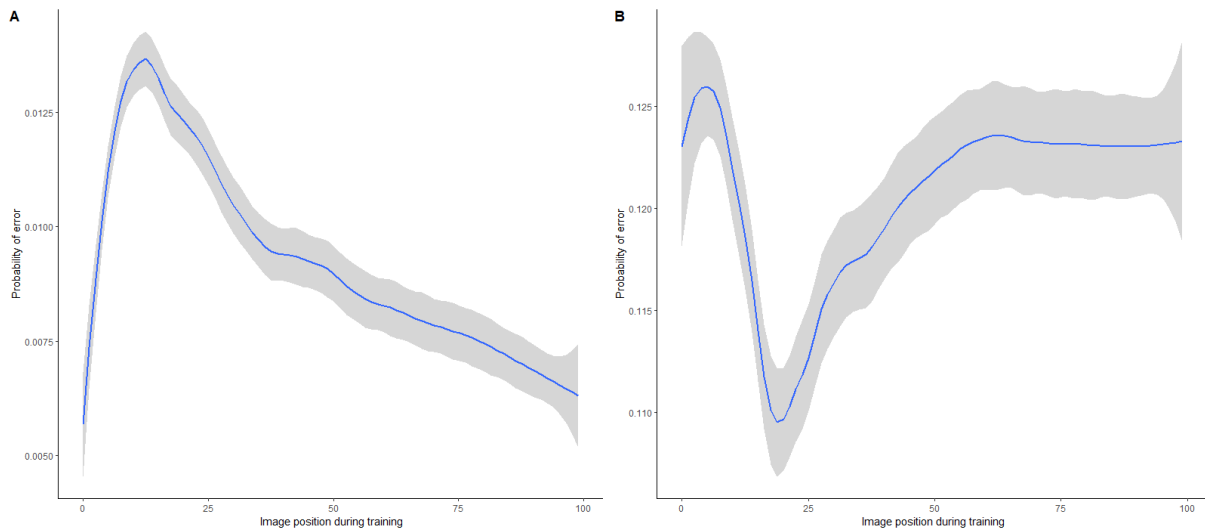
854

855 **Figure 4.** Results from the reproduction of Standing's experiment. (A) Number of images  
 856 retained by the model as a function of the number of the dataset size during training ( $\log_{10}$  scale)  
 857 (B) The probability of error as a function of the number of images learned during training. Red  
 858 curves: Standing's behavioral data (Standing, 1973). Blue curves: performance for the anti-  
 859 Hebbian solution. Green curves: performance for the Hebbian solution.



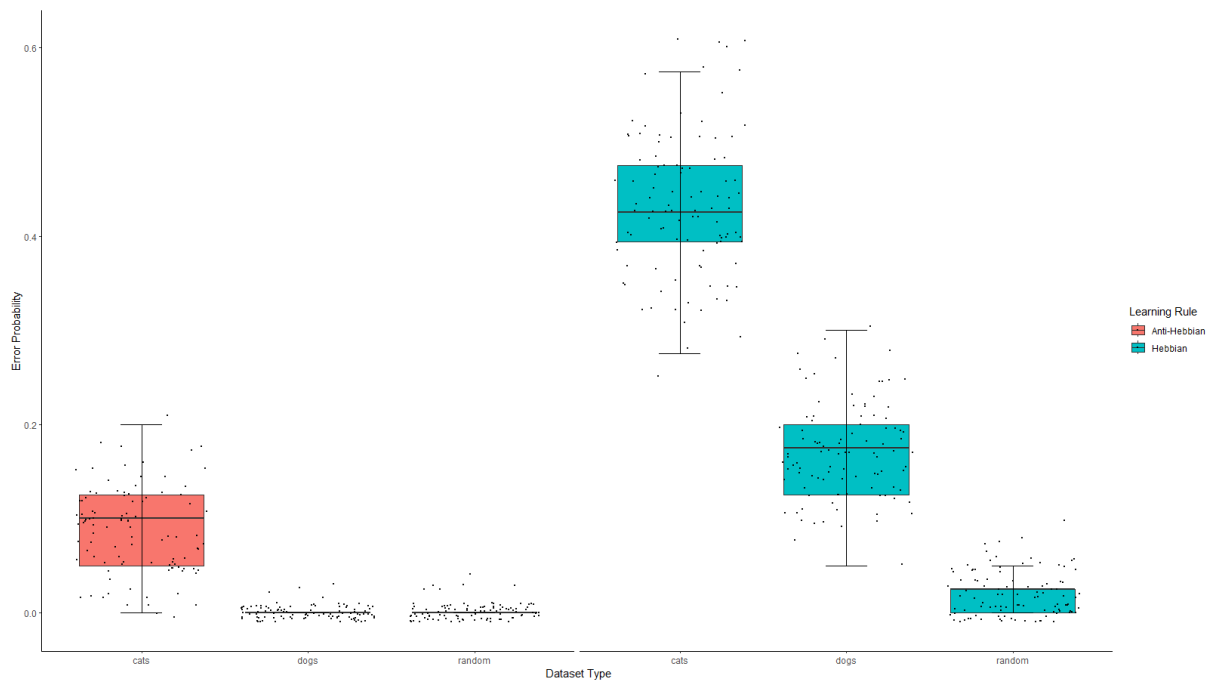
860

861 **Figure 5.** Mean probability of error for a given image and standard deviation (grey areas) as a  
862 function of the position of this image in the training phase ( $N = 100$ ). (A) Performance tested  
863 with the anti-Hebbian model. (B) Performance tested with the Hebbian model.



864

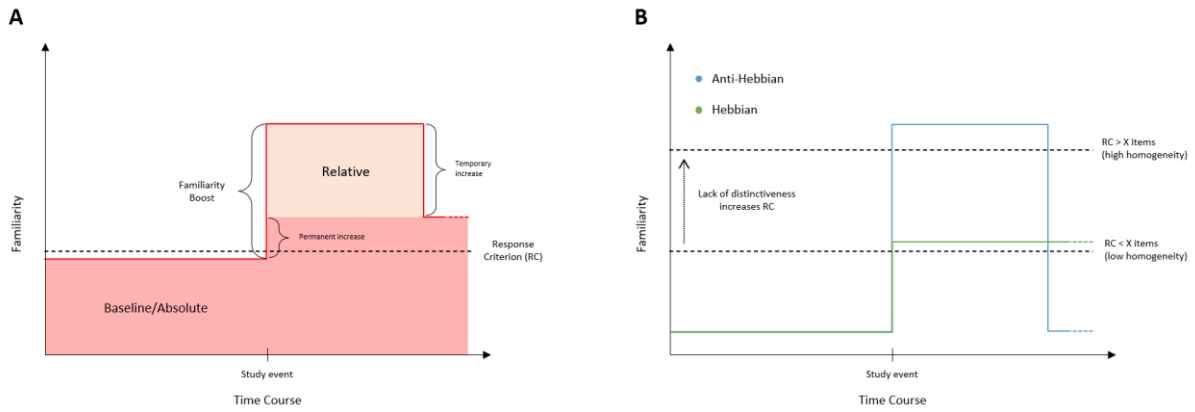
865 **Figure 6.** Mean probability of error and standard deviation when the two models are tested on  
866 dataset with different homogeneity levels ( $N = 40$ ).



867



868 **Figure 7.** Time course of the familiarity signal. (A) Collective contribution of both absolute  
 869 and relative familiarity to the familiarity decision as described in Coane et al. (2011). (B)  
 870 Separate contributions of the absolute familiarity as modeled by the Hebbian learning rule  
 871 (green curve) and the relative familiarity as modeled by the anti-Hebbian learning rule (blue  
 872 curve) under different level of distinctiveness.



873